Electrode and Substrate Contacts in Carbon Nanofiber Interconnects

Tsutomu Saito, Hisashi Yabutani, Toshishige Yamada, Patrick Wilhite, and Cary Y. Yang

Center for Nanostructures, Santa Clara University
500 El Camino Real,
Santa Clara, California 95053, USA
Phone:+1-408-554-6817, Fax:+1-408-554-5474, E-mail: Tsaito1@scu.edu

Abstract

To study the reliability of carbon nanofiber (CNF) interconnect under high-current stress, electrical and thermal transports across CNF-electrode interfaces and between electrodes are considered. For this investigation, three different types of contacts are examined: (a) CNF-Au electrode, (b) CNF-SiO_2 substrate, and (c) tungsten-deposited CNF-Au electrode. We have determined that contact (c) improves the overall electrical and thermal transport characteristics of the system.

Introduction

Carbon nanostructures such as carbon nanotubes (CNTs) [1] and carbon nanofibers (CNFs) [2] have been investigated for next-generation on-chip interconnect applications [3] because of their high current capacity and excellent electrical and thermal properties. To properly exploit these properties for such applications, the electrothermal behavior must be carefully scrutinized. Recent studies of thermal and electrical transport in carbon nanostructures [4-9] demonstrated that breakdown is related to Joule heating along the length of the nanofiber. Our previous work suggested that the electrode and substrate contacts are critical determining factors for optimal interconnect performance [8-9]. The results showed that current stressing mainly improves the electrode contacts, and if the fabricated contacts are already electrically and thermally optimal, there is little room for further improvement from current stressing on the entire structure [9]. Also, unlike the case of CNF drop-cast on Au electrodes, the CNF bulk resistance is not affected by current stressing except at breakdown for devices with W-Au electrodes [9]. This paper extends the study further and focuses on examining the roles of these two CNF-electrode contacts, as well as the role of substrate contact on the pre-breakdown behavior of this model horizontal interconnect system.

Experiment

We report the behavior of CNFs under high-current stress, where CNF-electrode contact plays a critical role. Three different contacts types are considered, as shown in Figure 1. These are: (1) CNF-Au electrode contact; (2) CNF-SiO_2 substrate contact; and (3) tungsten-deposited CNF-Au electrode contact. CNFs were grown using plasma-enhanced chemical vapor deposition (PECVD) with a Ni catalyst layer on Si substrate [2]. Each CNF consists of a stacked-cone structure surrounded by one or more cylindrical graphene walls. These test structures were prepared by dispersing CNFs in an isopropyl alcohol solution onto a substrate of pre-patterned Au electrodes on an oxidized silicon wafer. The test structure thus formed has not only high contact resistance between CNF and electrode but also its total resistance spans a wide range, generally from 0.1 to 10MΩ. This is due to structural variations at the interface between CNF and electrode, as well as the condition of the electrode itself. To resolve this problem, we deposit W onto the CNF-electrode contact, using a focused ion beam system with source gas $W(CO)_6$. Details of this procedure have been reported [9]. Electrical measurement was then

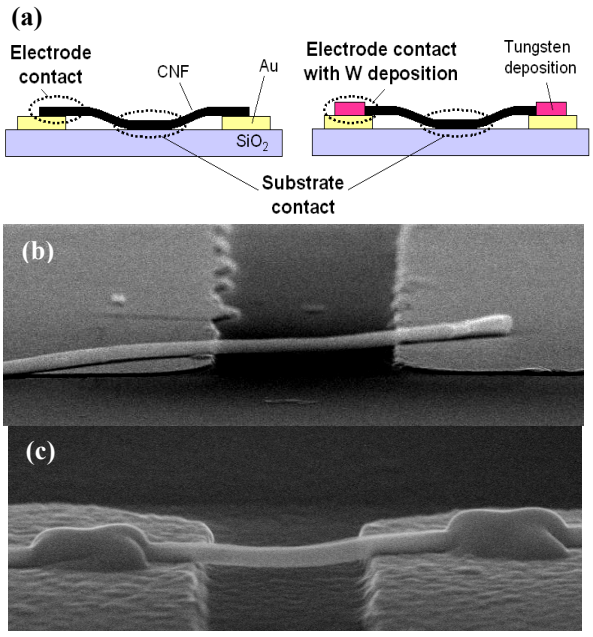

Figure 1. (a) Schematic diagram for three different contacts to CNF. (b) SEM image of a CNF interconnect test device on SiO_2 substrate, with CNF resting on Au electrodes. (c) SEM image of a test device with W deposited on CNF-Au electrode contacts.

performed to examine the behavior prior to breakdown from constant-current stressing [8-9]. Here we present results for several devices with CNFs ranging from 100 to 200 nm in diameter and 1.5 to 8.6 μm in length.

Results and Discussion

In all experiments for CNFs suspended between two electrodes, we have demonstrated that breakdown always occurred near the middle of the nanofiber [8]. This is consistent with diffusive heat transport observed in CNTs at high bias [10], suggesting the importance of Joule heating in the CNF breakdown process.

Figure 2(a) shows typical SEM images before and after breakdown for a CNF partially supported on SiO_2 substrate with drop-cast Au electrodes. The suspended and substrate-supported segments are identified using a bright contrast imaging technique developed previously [11]. Clearly CNF segments contacted to the SiO_2 substrate or electrode can dissipate heat more effectively than suspended CNF segments. In this configuration, the CNF is usually not fully supported by either the substrate or the electrodes, and there can be more than one suspended segment. Nevertheless, breakdown always occurs near the middle of the longest suspended segment. Based on our previous analysis [8], this finding suggests that the efficiencies of heat dissipation through the substrate and electrode contacts are similar.

Figure 2(b) shows SEM images before and after breakdown for a CNF partially supported on SiO_2 substrate with W-deposited Au electrodes. The breakdown point in the suspended segment is closer to the substrate contact, away from the W-deposited contact. The same result is observed for all partially supported configurations with W-Au electrodes. This observation infers that the W-Au electrode has much more efficient thermal transport properties. Detailed electrothermal modeling has been performed to predict the breakdown location with respect to CNF contacts to the substrate and electrode, and the results are

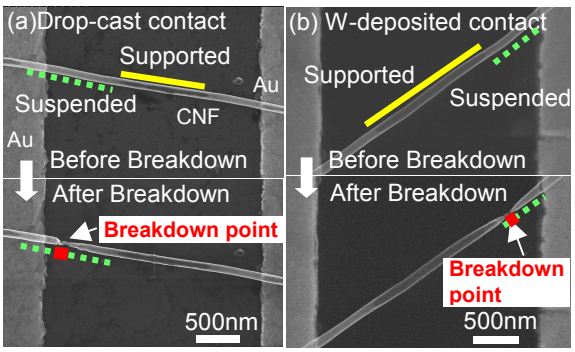

Figure 2. SEM images of CNF before and after breakdown: (a) drop-cast contact; (b) W-deposited contact.

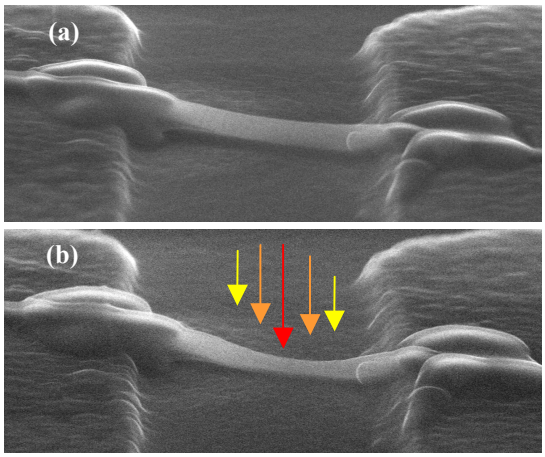

Figure 3. SEM images of CNF deformation due to electrical stress. (a) CNF test device before current stressing. (b) The same test device after stressing at 350μA.

consistent with observations [12].

Figure 3 shows SEM images of the test structure using a fully supported CNF on SiO_2 substrate between two W-Au electrodes. Figure 3(a) shows the pre-stress state for this test structure and Figure 3(b) shows the state after 350μA was applied for three minutes in ambient. In Figure 3(a), the CNT segment in contact with the substrate is uniform along its length. This observation suggests that the heat dissipation from the nanofiber to the substrate is also uniform. Because of this direct contact between CNF and substrate, and excellent heat dissipation at the W-Au contact, there is little structural change in this test device up to a stressing current of 325μA. At 350μA, however, the nanofiber is abruptly deformed, as shown in Figure 3(b), with the largest deformation near the middle of the nanofiber. This deformation continues until the CNF breaks down at 375μA. This observation is completely consistent with the predicted highest temperature at the middle of a symmetric device subject to current stressing [8,12]. It is also consistent with our previous hypothesis that prior to breakdown, partial evaporation of the nanostructure occurred due to Joule heating [7].

We have examined another test device consisting of a CNF with diameter similar to the one in Figure 3, partially supported by the substrate between two W-Au electrodes. Unlike the device in Figure 3, this device shown in Figure 4 is an asymmetric structure as there are two suspended segments of different lengths on either side of the supported segment. Figure 4(a) shows the pre-stress state of this test structure and Figure 4(b) shows the state after 100μA was applied for 3 minutes in ambient. After current stressing, the contacted segment increases in length as shown in Figure 4(b), and breakdown occurs at 250μA. Thus, while the 100μA stressing current is insufficient to initiate

breakdown of the CNF, it nonetheless increases the fraction of segment in contact with the substrate. Further, by comparing this device with the one in Figure 3, the fact that this device only makes partial contact with the substrate (thus less efficient Joule heat dissipation) degrades its current capacity. Because of efficient heat dissipation at the W-Au electrode, Joule heating in this test device largely occurs along the CNF between the two electrodes. As in the device in Figure 2(b), the breakdown location (also the highest temperature point) moves from the middle of the suspended segment (as in a symmetric structure) towards the supported segment in this asymmetric structure.

Figure 4(c) shows the measured voltage (averaged over each stress cycle) as a function of stressing current for the test device in Figures 4(a) and (b). Below 100μA, the voltage varies almost linearly with current. Above 100μA, the voltage starts to taper off, and approaches saturation at high stressing current. While the maximum temperature in the nanofiber must increase with increasing stressing current (otherwise breakdown would not occur), the elongated supported segment shown in Figure 4(b) enhances heat dissipation. The decrease in resistance due to voltage decrease is likely a result of this enhanced heat dissipation. The resistance of this system can be characterized by a negative temperature coefficient, as the decrease in resistance with increasing stressing current is accompanied by increased Joule heat generation and increase in temperature.

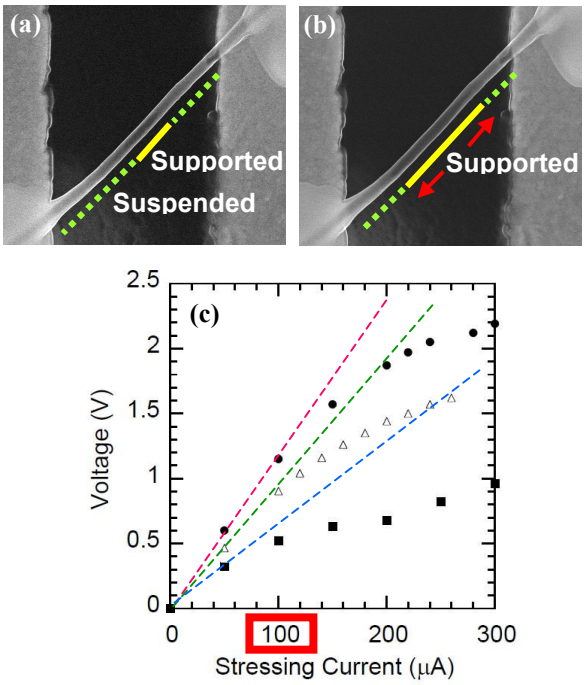

Figure 4. Changes in CNF test device due to electrical stress. SEM images of the CNF test structure (a) before current stress and (b) after stressing at 100 μA. (c) Observed average voltage as a function of stressing current.

Conclusion

It is demonstrated experimentally that Joule heat dissipation through various contacts in a CNF interconnect test structure holds the key in determining the performance and reliability of the device. W-deposited electrodes have been shown to dissipate heat efficiently, while CNF contact to the substrate plays an important role in determining the current capacity and breakdown location. The results obtained here provide an enhanced understanding of the electrothermal transport and breakdown mechanisms in carbon nanofiber interconnects.

References

[1] J. Li, Q. Ye, A. M. Cassell, H. T. Ng, R. Stevens, J. Han, and M. Meyyappan, *Appl. Phys. Lett*. **82**, 2491 (2003).

[2] Q. Ngo, A. M. Cassell, A. J. Austin, J. Li, S. Krishnan, M. Meyyappan, and C. Y. Yang, *IEEE Electron Device Lett*. **27**, 221 (2006).

[3] W. Hoenlein, F. Kreupl, G. S. Duesberg, A.P.Graham, M. Liebau, R.V. Seidel, and E. Unger, *IEEE Transactions on components and packaging technologies*, Vol.**27**, No.4, 629, (2004)

[4] J. Y. Huang, S. Chen, S. H. Jo, Z. Wang, D. X. Han, G. Chen, M. S. Dresselhaus, Z. and F. Ren, *Phys. Rev. Lett.* **94**, 236802 (2005).

[5] T. D. Yuzvinsky, W. Mickelson, S. Aloni, S. L. Konsek, A. M. Fennimore, G. E. Begtrup, A. Kis, B. C. Regan, and A. Zettl, *Appl. Phys. Lett*. **87**, 083103 (2005).

[6] E. Pop, D. A. Mann, J. Cao, K. E. Goodson, and H. Dai, *J. Appl. Phys*. **101**, 093710 (2007).

[7] M. Suzuki, Y. Ominami, Q. Ngo, C. Y. Yang, J. Li, and A. M. Cassell, *J. Appl. Phys*. **101**, 114307 (2007).

[8] H. Kitsuki, T. Yamada, D. Fabris, J. R. Jameson, P. Wilhite, M. Suzuki, and C. Y. Yang, *Appl. Phys. Lett*. **92**, 173110 (2008).

[9] T. Saito, T. Yamada, D. Fabris, H. Kitsuki, P. Wilhite, M. Suzuki, and C. Y. Yang, *Appl. Phys. Lett*. **93**, 102108 (2008)

[10] E. Pop, D. Mann, J. Cao, K. Goodson, and H. Dai, *Phys. Rev. Lett.* **95**, 155505 (2005).

[11] M. Suzuki, Y. Ominami, Q. Ngo, C. Y. Yang, T. Yamada, A. M. Cassell, and J. Li, *J. Appl. Phys.* **100**, 104305 (2006).

[12] T. Yamada, T. Saito, D. Fabris, and C. Y. Yang, "Electrothermal Analysis of Breakdown in Carbon Nanofiber Interconnects", submitted for publication.